

# Molecular docking studies on quinazoline antifolate derivatives as human thymidylate synthase inhibitors

Vivek Srivastava<sup>1,4</sup>, Satya Prakash Gupta<sup>2</sup>, Mohd. Imran Siddiqi<sup>3</sup> and Bhartendu Nath Mishra<sup>4\*</sup>

<sup>1</sup>Department of Biotechnology, Meerut Institute of Engineering & Technology, Meerut-250005; <sup>2</sup> Department of Pharmaceutical technology, Meerut Institute of Engineering & Technology, Meerut-250005; <sup>3</sup>Computational Biology and Bioinformatics Lab., MSB Division, Central Drug Research Institute; Lucknow- 226001; <sup>4</sup>Department of Biotechnology, Institute of Engineering & Technology, UP Technical University, Sitapur Road, Lucknow 226021. Bhartendu Nath Mishra – E-mail: profbnmishra@gmail.com; Phone:+ 91-9415012030; + 91-522 – 2365730;

\*Corresponding Author

Received October 30, 2009; Accepted November 15, 2009; Published February 28, 2010

## Abstract:

We have performed molecular docking on quinazoline antifolates complexed with human thymidylate synthase to gain insight into the structural preferences of these inhibitors. The study was conducted on a selected set of one hundred six compounds with variation in structure and activity. The structural analyses indicate that the coordinate bond interactions, the hydrogen bond interactions, the van der Waals interactions as well as the hydrophobic interactions between ligand and receptor are responsible simultaneously for the preference of inhibition and potency. In this study, fast flexible docking simulations were performed on quinazoline antifolates derivatives as human thymidylate synthase inhibitors. The results indicated that the quinazoline ring of the inhibitors forms hydrophobic contacts with Leu192, Leu221 and Tyr258 and stacking interaction is conserved in complex with the inhibitor and cofactor.

**Keywords:** Human thymidylate synthase, Quinazoline antifolate derivatives and Molecular docking.

## Background:

Thymidylate synthase has been a primary target for chemotherapy aimed at cancers of the gastrointestinal tract and head and neck [1] despite moderate response in 30-40% of patients. Thymidylate synthase has been favorite target for designing and developing inhibitors which could be used as anticancer drugs [2]. A major problem affecting TS-directed treatments is that tumor cells often react to an exposure to Thymidylate synthase inhibitors by raising levels of intracellular TS activity about 2- to 4-fold, which may lead to resistance. Thymidylate synthase (TS) catalyzes the reductive methylation of 2'-deoxyuridine 5'-monophosphate (dUMP) to thymidine 5'-monophosphate (dTMP), using the co-substrate, 5,10-methylenetetrahydrofolate (CH<sub>2</sub>H<sub>4</sub>folate) as a one-carbon donor and reductant. The physical structures of bacterial TSs have been relatively well defined, and crystallographic data, in concert with data derived from kinetic, spectroscopic, and site-directed mutagenesis studies, have led to a detailed understanding of the catalytic mechanism of these enzymes [3]. In contrast, relatively few investigations of mammalian TS structure and catalysis have been conducted. The three-dimensional structure of the native human thymidylate synthase (hTS) has been reported previously [4]. The data showed a surprising feature not observed in TSs from other sources: loop 181-197 containing the catalytic cysteine, Cys-195, was in an inactive conformation, and rotated ~ 180° with respect to its orientation in bacterial TSs, with the sulfhydryl of Cys-195 over 10 Å from the location of sulfhydryls of corresponding cysteine residues in bacterial enzymes. Subsequent determination of the structure of a ternary inhibitory complex between closely related ratTS (rTS) and dUMP and tomudex [5] has shown that the ligands bind to the enzyme in the active conformation. Recently, it was found that also in the hTS-dUMP-tomodex complex hTS is in the active conformation. The inactive conformation has not been observed in TSs other than human [6].

Although T S does not represent a new target, there is still enthusiasm for the development of quinazoline derivatives. A unique feature of TS is the selectivity that is possible in the design of inhibitors. This makes it an ideal "old" target for rational and effective drug design for anticancer agents. Nowadays, molecular docking approaches are routinely used in modern drug design to help understand drug-receptor interaction. It has been shown in the literature that these computational techniques can strongly support and help the design of novel, more potent inhibitors by revealing the mechanism of drug-receptor

interaction [7]. However, so far, there has been no report concerning the application of molecular docking methodology for understanding the binding of quinazoline antifolate derivatives. The antifolate compounds evaluated in this investigation are derivatives of quinazoline antifolate, having structures similar to the tomudex/ZD1694 class of antifolates, where quinazoline is a compound made up of two fused six-membered simple aromatic ring, a benzene ring and a pyrimidine ring. Its chemical formula is C<sub>8</sub>H<sub>6</sub>N<sub>2</sub>. Due to an interest in new anticancer drugs, several quinazoline antifolate inhibitors were chosen from the ICI Pharmaceutical & Institute of Cancer Research, England for screening against human thymidylate synthase [8-11].

Molecular docking is a key tool in structural molecular biology and computer-assisted drug design. The goal of ligand-protein docking is to predict the predominant binding model(s) of a ligand with a protein of known three-dimensional structure. In this study, we have used fast flexible docking to study the binding orientations and predict binding affinities of quinazoline antifolate derivatives. Such studies have been carried out to understand the forms of interaction of one hundred six compounds, synthesized by Marsham *et al* [8-11] for the human thymidylate synthase. The results obtained from this study would be useful in both understanding the inhibitory mode of quinazoline antifolate derivatives as well as in rapidly and accurately predicting the activities of newly designed inhibitors on the basis of docking scores. These models also provide some beneficial clues in structural modification for designing new inhibitors for the treatment of cancer with much higher inhibitory activities against thymidylate synthase.

## Methodology:

### Molecular structures & optimization

The biological activity data of quinazoline antifolate derivatives (one hundred six compounds), reported by Marsham *et al* [8-11] was used in the present study shown in Table 1. The structures of all the compounds were constructed using the InsightII 2000.1 Builder module (<http://www.accelrys.com>). The geometries of these compounds were subsequently optimized using Discover module of InsightII 2000.1 using CVFF force field. The structure of humanTS protein (PDBid code 1100) was obtained from Protein Data Bank (<http://www.rcsb.org>).

### Molecular docking

Molecular docking of quinazoline antifolate derivatives to the active site of human thymidylate synthase was carried out using modern docking engine LigandFit available with Cerius2\_4.9 (<http://www.accelrys.com>). This algorithm makes use of a cavity detection algorithm for detecting invaginations in the protein as potential active site regions. A shape comparison filter is combined with a Monte Carlo conformational search for generating ligand poses consistent with the active site shape. Candidate poses are minimized in the context of the active site using a grid-based method for evaluating protein-ligand interaction energies. The docking was carried out with the following non default settings in LigandFit: site partitioning in order to fully access the potential docking orientation of the active site, maximum trials variable table values to help the pseudorandom conformational analysis, and the CFF force field [12] option used for the grid energy calculations. The flexible fitting option was selected for generation of alternative conformations on the fly, as was the diverse conformer's option to ensure the solutions generated cover a broad range of conformations with similar low-energy docking scores, and a maximum of 30 top scoring diverse ligand poses were returned for each of the compounds.

### Scoring function

The docked conformations were further scored using different scoring functions available with Cerius2 [12]. The LigandFit algorithm [13] uses an internal scoring function, DockScore, to select and return dissimilar poses for each compound. DockScore is a simple force field based scoring function which estimates the energy of interaction by summing the ligand/protein interaction energy and the internal energy of the ligand. CFF force field [12] was used to resolve the van der Waals parameters for DockScore. The top DockScore pose was used for postdocking scoring. Scoring was performed using a set of scoring functions as implemented in Cerius2 [12]. These included LigScore1, LigScore2,-PLP1,-PLP2, - JAIN, PMF, LUDI and DockScore available from the docking process. The putative 3D poses and score results were then stored as an SD file. Each docking was minimized, using DockScore, the only purely molecular mechanics based scoring function employed in this study, and this minimized pose was then presented to each of the other scoring functions, which were either knowledge based or regression based.

### Protein preparation

The high-resolution (2.50 Å) X-ray structure of human thymidylate synthase complex with tomudex (PDBid code 1100) was imported into Cerius2 [12], and the ligand was extracted to leave a cavity. Docking simulations were carried out with substrate dUMP and without water molecules, to elucidate the role of dUMP for the binding of quinazoline antifolate derivatives.

### Hardware and software

Insight II 2000.1 [<http://www.accelrys.com>] and Cerius2 [12] were used for molecular modeling on a SGI Origin 300 workstation equipped with 4 \* 600 Mhz R12000 processor.

### Results and Discussion:

To date, several crystal structure of human thymidylate synthase in complex with different inhibitors have been reported *viz* 1100 with ternary complex with dUMP and tomudex, [14], 1JUJ with dUMP LY231514, a pyrrolo(2,3-d)pyrimidine-based antifolate [15], 1JTQ with dUMP and the pyrrolo(2,3-d)pyrimidine-based antifolate LY341770 [15], 1JU6 with dUMP and LY231514, a pyrrolo(2,3-d)pyrimidine-based antifolate [15], 1HVV with dUMP and raltitrexed, an antifolate drug [16] etc. which provide information about the exact location and composition of inhibitor binding pocket and opportunity to use the enzyme in a functional conformation. We used X-ray structure of human thymidylate synthase in ternary complex with dUMP and tomudex (PDBid code 1100) for the docking study.

### Validation of the docking method

To ensure that the ligand orientation and the position obtained from the docking studies were likely to represent valid and reasonable binding modes of the inhibitors, the LigandFit program docking parameters had to be first validated for the crystal structure used (PDBid 1100). The ligand tomudex, in the conformation found in the crystal structure, was extracted and docked back to the corresponding binding pocket, to determine the ability of LigandFit to reproduce the orientation and position of the inhibitor observed in the crystal structure. Results of control docking showed that LigandFit determined the optimal orientation of the docked inhibitor, tomudex to be close to that of the original orientation found in the crystal shown in **Figure 1(a)**. The low RMS deviation of 0.290 Å between the docked and crystal ligand coordinates indicate very good alignment of the experimental and calculated positions especially considering the resolution of the crystal structure (2.50Å).

### Interaction modes between the quinazoline antifolate derivatives and human thymidylate synthase

To study the binding modes of quinazoline antifolate derivatives in the binding site of human thymidylate synthase, intermolecular flexible docking simulations were performed by means of LigandFit program and Dockscores were calculated from the docked conformations of the human thymidylate synthase-inhibitor complexes. All the compounds in the dataset were docked into the active site of human thymidylate synthase, using the same protocol. Thymidylate synthase monomer consists of an  $\alpha/\beta$ -fold containing 7  $\alpha$ -helices and 10  $\beta$ -strands, arranged in three layers : a six stranded mixed  $\beta$ -sheet, a long  $\alpha$ -helix across the sheet flanked by two shorter helices, and a mixed layer containing the remaining four helices and two antiparallel two-stranded  $\beta$ -sheets. The large  $\beta$ -sheets from the monomers stack against each other to form dimer interface. The dimer contains two active sites, one within each monomer. The active site of human Thymidylate Synthase comprises of amino acids residues such as Arg50, Phe80, Leu 108, Asn112, Leu192, Asp218, Gly220, Leu221, Gly222, Phe225 and Tyr258. As most of the amino acid residues in the active site are hydrophobic so they are involved in strong hydrophobic interactions with the quinazoline antifolate derivatives. It was depicts the aligned binding conformations of the quinazoline antifolate derivatives in the binding pocket of the human thymidylate synthase, which were derived from the docking simulations by LigandFit software. Molecular docking studies of quinazoline antifolate derivatives into human thymidylate synthase binding site revealed very clear preference for the binding pocket. All of the inhibitors occupy the binding site well as seen from the **Figure 2**.

The majority of the contacts between the quinazoline antifolate derivatives and the protein are non polar, making use of the hydrophobic side chains in the binding site. Most of the quinazoline antifolate derivatives bind in more or less similar fashion with its quinazoline ring occupying the interior of the deep cleft and their tail is extended towards the entrance of the hydrophobic binding cavity. The quinazoline ring of quinazoline antifolate derivatives therefore bind to the human thymidylate synthase active site in an identical fashion, as reported in case of other inhibitors like tomudex [14] and raltitrexed [16]. The quinazoline ring of the inhibitors forms hydrophobic contacts with Leu192, Leu221 and Tyr258. As seen from our docking studies the quinazoline core occupies the same core in the binding site as does the quinazoline ring of tomudex and makes stacking interaction with pyrimidine ring of UMP. This stacking interaction is very important and has been conserved in all the thymidylate synthases for with crystal structures has been solved in complex with the inhibitor and cofactor. **Figure 1(b)** represents the binding conformations of the highly active compounds, all of which share the common binding mode with quinazoline core occupy space deep in the cavity and ester tail extends towards the solvent.

The binding mode of the most active comp32 has been shown in **Figure 1 (c)**. As expected, comp32 bind to the thymidylate synthase active site in the similar conformation as other known TS inhibitors (tomudex, raltitrexed etc.) which mainly bind using the quinazoline moiety and this moiety is presented to pyrimidine ring of cofactor UMP. This pterin ring is involved in  $\pi$ - $\pi$  stacking interactions with the pyrimidine ring of UMP. This stacking interaction is very important and has been conserved in most the thymidylate synthases for which crystal structures have been solved with UMP and inhibitors in ternary complex with the enzyme. The amino group substituted at quinazoline ring of comp32 makes significant hydrogen bonding interaction with side chain oxygen of Tyr258 and sugar oxygen atom of cofactor UMP. So it can be concluded that the presence of a hydrogen bond donor group at 2-position of the quinazoline moiety is important for thymidylate synthase activity of the inhibitors. In addition to this important hydrogen bonding interaction quinazoline ring nitrogen N3

and quinazoline carbonyl group make hydrogen bond with backbone oxygen of Asp218 and backbone nitrogen of Gly222 respectively. In addition to these hydrogen bonding interaction Comp32 is involved in van der Waals interactions through its phenyl ring with Ile108 and Phe225. Quinazoline ring is also involved in van der Waals interactions with the Trp109 (Residue not shown in figure for clarity) and Leu221 of the protein. Phe80 also show stacking interactions with the glutamyl chain of Comp32 and these particular interactions play very important role in thymidylate inhibition and need to be present for good inhibition by the inhibitors. Comp32 shows all the interactions shown by the well known potent inhibitor tomudex of thymidylate and binds in almost the same fashion as tomudex do, however comp32 show additional hydrogen bonding interaction via  $-NH_2$  substituted at quinazoline moiety (**Figure 1(c)**) instead of tomudex which has methyl group substituted at this position.

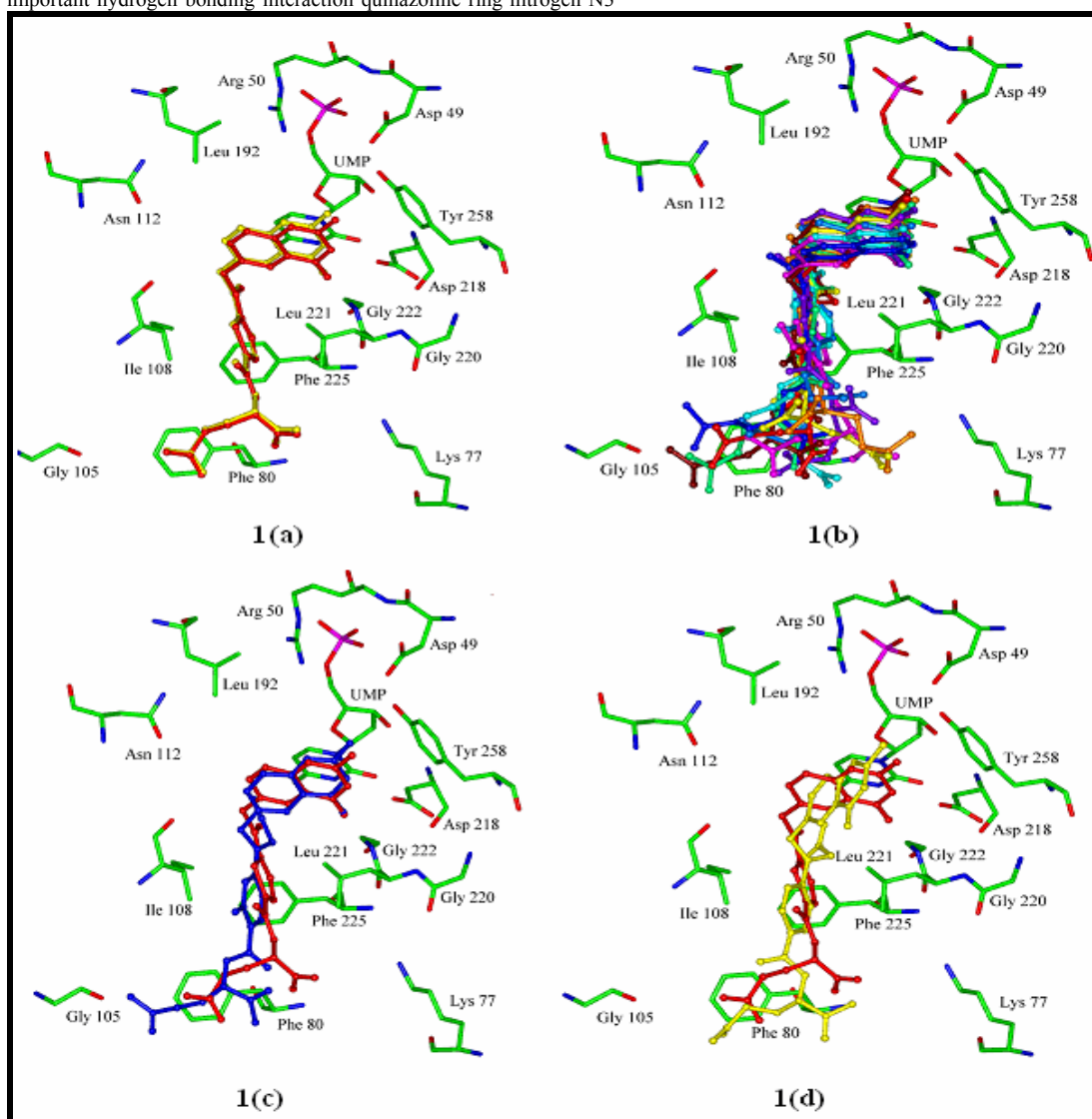


**Figure 1:** (a) Conformation of tomudex crystal structure (red) as compared to the docked conformation of tomudex (yellow) with cofactor substrate dUMP (atom color). Amino acid residues are presented by atom color, (b) Docked conformation highly active compounds (i) comp32 (brown) (ii) comp47 (red) (iii) comp31 (orange) (iv) comp35 (yellow) (v) comp1 (green blue) (vi) comp52 (cyan) (vii) comp50 (light blue) (viii) comp34 (blue) (ix) comp37 (violet) (x) comp76 (magenta), (c) Docked confirmation of comp32 compared with binding mode of tomudex, 1(d) Docked confirmation of comp13 compared with binding mode of tomudex and it shows the binding mode of least active comp13 and its comparison with the binding of tomudex.

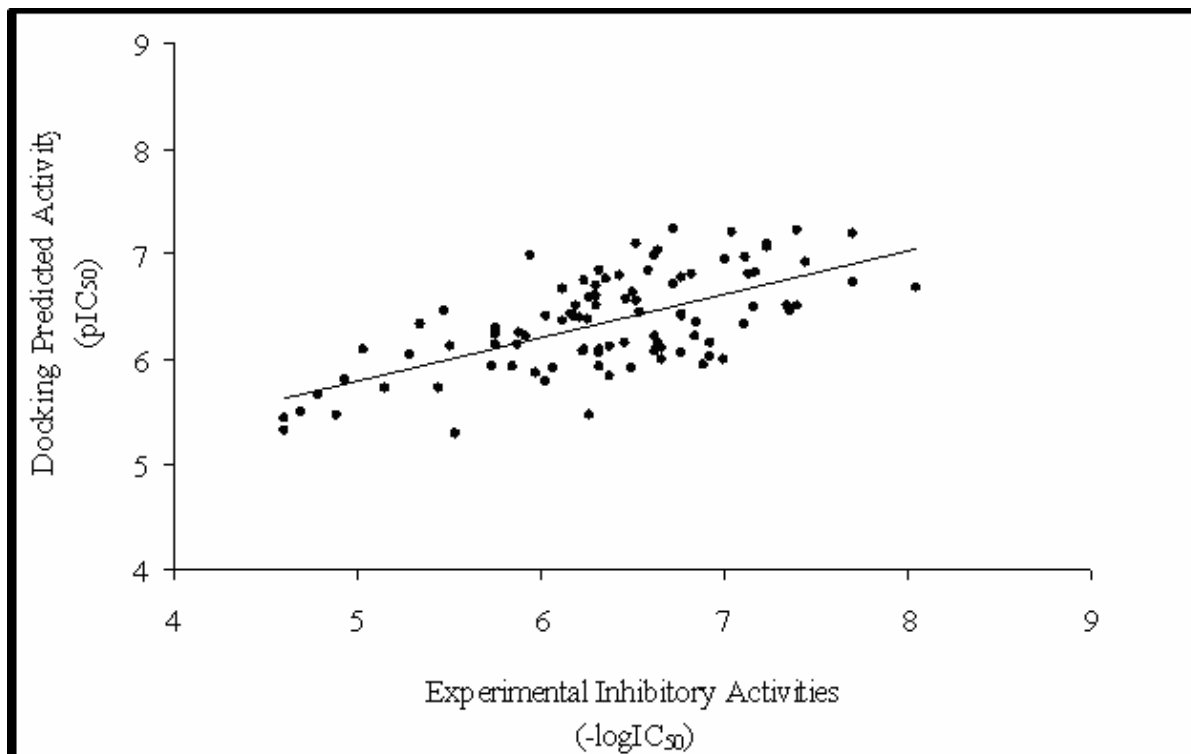


**Figure 2:** A correlation for binding conformations and binding models of the quinazoline antifolate derivatives with human thymidylate synthase.

Comp13 bind to thymidylate synthase active site in slightly tilted (about 45%) way when compared to the binding of highly active comp32 and crystal structure ligand tomudex. This particular tilt in the binding may be contributed by the absence of the hydrogen bonding amino group substituted at 2-position of the quinazoline ring. Additionally, this hydrogen bond positions the inhibitors for stacking interactions with the pyrimidine ring of the cofactor UMP. Loss or decrease in the stacking interaction may lead to decreased affinity for the protein binding site. The phenyl ring in comp13 is unsubstituted whereas fluorine atom is substituted at 3-position of highly active comp32 which may lead to decreased van der Waals interactions with Ile108 and Phe225 and hence lead to decreased activity in case of comp13 and other inactive compounds.

#### Correlation between docking scores and inhibitory activity

An important application of LigandFit docking program in structure-based drug design is to predict the inhibitory activities while determining the binding conformation of an inhibitor with the target by making use of their dock scores. Linear regression analysis analyses were performed to explore whether the docking scores could be correlated with the experimental activities. The predicted inhibitory activity of quinazoline antifolate derivatives as inhibitors on the basis of dock score is listed in **Table 1** (see **supplementary material**). Linear regression analysis analyses were performed to explore whether the docking scores could be correlated with the experimental activities. The equation was obtained for the inhibitory activities represented as  $pIC_{50}$  values, using the Dock score, Ligscore1, Ligscore2, -PLP1, -PLP2, JAIN, -PMF and Consensus score as the variable descriptors. A model with the correlation coefficient ( $r^2$ ) of 0.148 was obtained for one hundred six compounds. Removal of 10 compounds (comp2, comp22, comp25, comp27, comp35, comp48, comp65, comp104, comp105, comp106) identified as outliers from the docking dataset yield a better model with correlation of coefficient ( $r^2$ ) of 0.494 was obtained for ninety six compounds. This rather good correlation demonstrates that the binding conformations and binding models of

the quinazoline antifolate derivatives with human thymidylate synthase are reasonable shown in **Figure 2**.

#### Conclusion:

The orientation of the quinazoline antifolate derivatives in the model complex is similar to that observed in the crystal structure. Despite some relaxation, due to the nature of the forcefield potentials, all important ligand-protein interactions are preserved during the energy minimization. Using the CVFF forcefield, the stacking interaction and hydrophobic contacts is very important in human thymidylate synthase complex with the quinazoline antifolate inhibitor and cofactor.

In this study, the molecular docking was applied to explore the binding mechanism and to correlate its docking score with the activity of a quinazoline antifolate derivatives. To our knowledge, this is the first study aimed at deriving docking studies for quinazoline antifolate derivatives. The docking studies provided good insights into the binding of quinazoline antifolate derivatives at the molecular level. Significant study between active sites and quinazoline antifolate derivatives will be analyzed to propose structural changes in these compounds, with the aim of rendering them more selective and thereby better human thymidylate synthase inhibitors.

#### Acknowledgement:

One of the authors, Mr. Vivek Srivastava is thankful to Council of Scientific and Industrial Research (CSIR), New Delhi for providing the Senior Research Fellowship (SRF) for carrying out the research work, Mr. Ashutosh Kumar for providing help in many ways for completion of this research work.

#### References:

- [1] YM Rustum *et al.*, *J. Clin. Oncol.* (1997) **15**: 389 [PMID: 8996166]
- [2] S Agrawal *et al.*, *J. Mol. Microbiol. Biotechnol.* (2003) **6**: 67 [PMID: 15044825].

- [3] CW Carreras *et al.*, *Annu. Rev. Biochem.* (1995) **64**: 721 [PMID: 7574499]
- [4] CA Schiffer *et al.*, *Biochem.* (1995) **34**:16279.
- [5] RR Sotelo-Mundo *et al.*, *Biochem.* (1999) **38**:1087.
- [6] J Phan *et al.*, *Journal of Biolo. Chem.* (2001) **276**:14170.
- [7] V Srivastava *et al.*, *Bioinformation* (2008) **3**: 180 [PMID: 19238244].
- [8] LR Hughes *et al.*, *Journal of Med. Chem.*(1990) **33**: 3060.
- [9] AL Jackman *et al.*, *Journal of Med. Chem.* (1990) **33**: 3067.
- [10] PR Marsham *et al.*, *Journal of Med. Chem.* (1990) **33**: 3072.
- [11] PR Marsham *et al.*, *Journal of Med. Chem.* (1991) **34**: 1594.
- [12] Cerius2 Version 4.10, Accelrys Inc., C. A. San Diego, <http://www.accelrys.com>.
- [13] CM Venkatachalam *et al.*, *J. Mol. Graph Model* (2003) **21**: 289 [PMID: 12479928]
- [14] R Almog *et al.*, *Protein Sci.* (2001) **10**: 988 [PMID: 11316879].
- [15] PH Sayre *et al.*, *J.Mol.Biol.* (2001) **313**: 813 [PMID: 11697906].
- [16] J Phan *et al.*, *Biochem.* (2001) **40**: 1897.

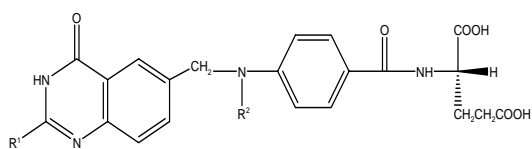
Edited by P. Kanguane

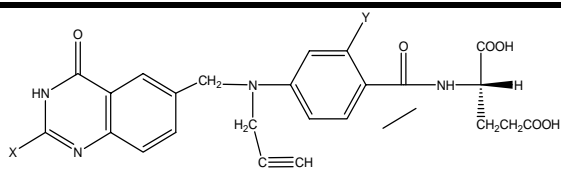
Citation: Srivastava *et al.*, *Bioinformation*, 4(8): 357-365 (2010)

**License statement:** This is an open-access article, which permits unrestricted use, distribution, and reproduction in any medium, for non-commercial purposes, provided the original author and source are credited.

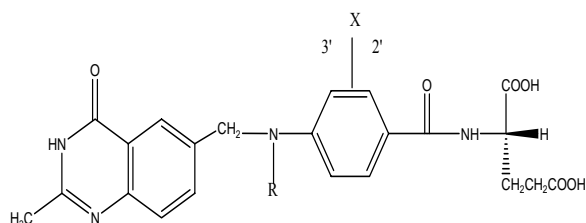
Supplementary material:

Table 1: Quinazoline antifolate derivatives with modifications

Quinazoline antifolate derivatives with modifications						
Derivative			Experimental Activity (pIC <sub>50</sub> )	Predicted Activity (pIC <sub>50</sub> )	Residual	DOCK SCORE
	Position R <sup>1</sup>	Position R <sup>2</sup>				
Comp1	CH <sub>3</sub>	CH <sub>2</sub> C≡CH	7.398	7.223	0.175	62.0985
<b>*Comp2</b>	<b>CH<sub>3</sub></b>	<b>H</b>	<b>5.35</b>	*****	*****	*****
Comp3	CH <sub>3</sub>	CH <sub>3</sub>	6.523	6.554	-0.031	74.1296
Comp4	CH <sub>3</sub>	CH <sub>2</sub> CH <sub>3</sub>	6.77	6.417	0.353	70.5759
Comp5	CH <sub>3</sub>	CH <sub>2</sub> CH=CH <sub>2</sub>	6.319	6.848	-0.529	54.0339
Comp6	CH <sub>3</sub>	(CH <sub>2</sub> ) <sub>2</sub> F	6.62	6.218	0.402	40.9059
Comp7	CH <sub>3</sub>	(CH <sub>2</sub> ) <sub>2</sub> Br	5.886	6.260	-0.374	55.3321
Comp8	CH <sub>3</sub>	(CH <sub>2</sub> ) <sub>2</sub> SH	5.754	6.261	-0.507	49.5824
Comp9	CH <sub>3</sub>	(CH <sub>2</sub> ) <sub>2</sub> OH	6.301	6.598	-0.297	79.1328
Comp10	CH <sub>3</sub>	(CH <sub>2</sub> ) <sub>3</sub> OH	6.268	5.477	0.791	34.8098
Comp11	CH <sub>3</sub>	(CH <sub>2</sub> ) <sub>2</sub> OCH <sub>3</sub>	4.789	5.661	-0.872	61.0809
Comp12	CH <sub>3</sub>	(CH <sub>2</sub> ) <sub>3</sub> OCH <sub>3</sub>	4.889	5.471	-0.582	41.3214
Comp13	CH <sub>3</sub>	CH <sub>2</sub> COCH <sub>3</sub>	4.602	5.437	-0.835	42.7647
Comp14	CH <sub>2</sub> CH <sub>3</sub>	CH <sub>2</sub> C≡CH	6.854	6.353	0.501	56.3263
Comp15	CH <sub>2</sub> CH <sub>3</sub>	H	4.699	5.504	-0.805	69.3533
Comp16	CH(CH <sub>3</sub> ) <sub>2</sub>	CH <sub>2</sub> C≡CH	6.208	6.394	-0.186	50.3742
Comp17	CH <sub>2</sub> F	CH <sub>2</sub> C≡CH	7.0	6.004	0.996	54.8555
Comp18	CH <sub>2</sub> F	CH <sub>3</sub>	5.535	5.297	0.238	56.1197
Comp19	CH <sub>2</sub> F	CH <sub>2</sub> CH <sub>3</sub>	6.432	6.801	-0.369	64.1659
Comp20	CH <sub>2</sub> F	(CH <sub>2</sub> ) <sub>2</sub> F	6.469	6.573	-0.104	59.3171
Comp21	CH <sub>2</sub> F	CH <sub>2</sub> C≡CH	6.237	6.744	-0.507	59.1139
<b>*Comp22</b>	<b>CF<sub>3</sub></b>	<b>CH<sub>2</sub>C≡CH</b>	<b>5.24</b>	*****	*****	*****
Comp23	CH <sub>2</sub> OH	CH <sub>3</sub>	6.194	6.512	-0.318	62.7282
Comp24	CH <sub>2</sub> OH	CH <sub>2</sub> CH <sub>3</sub>	6.585	6.836	-0.251	50.1905
<b>*Comp25</b>	<b>CH<sub>2</sub>OH</b>	<b>CH<sub>2</sub>CH=CH<sub>2</sub></b>	<b>6.04</b>	*****	*****	*****
Comp26	CH <sub>2</sub> OH	(CH <sub>2</sub> ) <sub>2</sub> F	6.658	6.113	0.545	58.132
<b>*Comp27</b>	<b>CH<sub>2</sub>OH</b>	<b>(CH<sub>2</sub>)<sub>2</sub>OH</b>	<b>6.11</b>	*****	*****	*****
Comp28	CH <sub>2</sub> NHCOCH <sub>3</sub>	CH <sub>2</sub> C≡CH	6.319	6.057	0.262	68.6361
Comp29	CH <sub>2</sub> S-2-pyrimidine	CH <sub>2</sub> C≡CH	6.62	6.990	-0.370	16.4223
Comp30	Phenyl	CH <sub>2</sub> C≡CH	6.658	5.994	0.664	44.0336

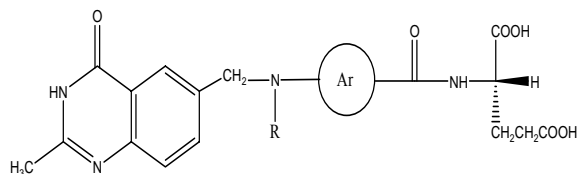


	Position X	Position Y				
Comp31	NH <sub>2</sub>	H	7.699	6.729	0.970	76.5712
Comp32	NH <sub>2</sub>	F	8.046	6.686	1.360	70.4486
Comp33	H	H	6.77	6.784	-0.014	51.1791
Comp34	H	F	7.237	7.100	0.137	70.4062
<b>*Comp35</b>	<b>CH<sub>3</sub></b>	<b>F</b>	<b>7.7</b>	<b>*****</b>	<b>*****</b>	<b>*****</b>
Comp36	CH <sub>2</sub> OH	H	7.009	6.959	0.050	63.9713
Comp37	CH <sub>2</sub> OH	F	7.237	7.063	0.174	65.219
Comp38	OCH <sub>3</sub>	H	7.167	6.498	0.669	71.557
Comp39	OCH <sub>3</sub>	F	7.444	6.929	0.515	55.4344



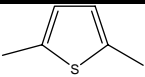
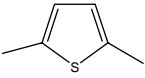
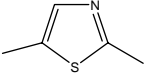
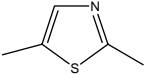
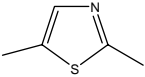
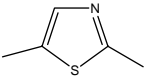
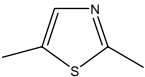
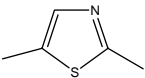
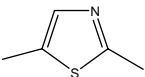
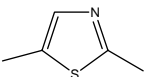
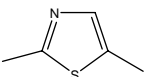
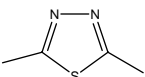
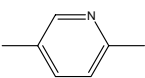
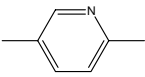
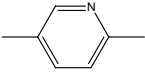
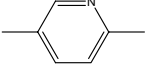
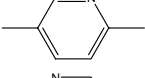
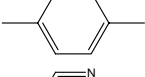
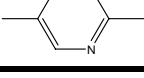
	Position X	Position R				
Comp40	H	H	5.347	6.337	-0.990	77.7392
Comp41	H	CH <sub>3</sub>	6.523	7.106	-0.583	61.9592
Comp42	H	CH <sub>2</sub> CH <sub>3</sub>	6.77	6.428	0.342	56.3273
Comp43	H	CH <sub>2</sub> CH=CH <sub>2</sub>	6.319	6.091	0.228	69.6427
Comp44	H	(CH <sub>2</sub> ) <sub>2</sub> F	6.62	6.070	0.550	49.2357
Comp45	H	(CH <sub>2</sub> ) <sub>2</sub> OH	6.301	6.703	-0.402	56.3914
Comp46	H	(CH <sub>2</sub> ) <sub>3</sub> OH	6.268	6.591	-0.323	48.7268
Comp47	2'-F	CH <sub>2</sub> C≡CH	7.699	7.199	0.500	60.0104
<b>*Comp48</b>	<b>2'-F</b>	<b>H</b>	<b>5.42</b>	<b>*****</b>	<b>*****</b>	<b>*****</b>
Comp49	2'-F	CH <sub>3</sub>	6.921	6.160	0.761	77.1705
Comp50	2'-F	CH <sub>2</sub> CH <sub>3</sub>	7.347	6.503	0.844	70.4267
Comp51	2'-F	CH <sub>2</sub> CH=CH <sub>2</sub>	7.119	6.965	0.154	41.9114
Comp52	2'-F	(CH <sub>2</sub> )F	7.367	6.464	0.903	60.3416
Comp53	2'-F	(CH <sub>2</sub> ) <sub>2</sub> OH	7.108	6.328	0.780	62.0603
Comp54	2'-F	(CH <sub>2</sub> ) <sub>3</sub> OH	6.229	6.074	0.155	53.2662
Comp55	2'-F	(CH <sub>2</sub> ) <sub>3</sub> NH <sub>2</sub>	4.931	5.808	-0.877	57.7233
Comp56	2'-F	CH <sub>2</sub> CN	6.77	6.058	0.712	53.4187
Comp57	2'-F	CH <sub>2</sub> CONH <sub>2</sub>	5.873	6.144	-0.271	62.2975
Comp58	3'-F	CH <sub>2</sub> C≡CH	5.845	5.933	-0.088	42.5697
Comp59	3'-F	H	5.03	6.085	-1.055	66.332
Comp60	3'-F	CH <sub>3</sub>	5.943	6.991	-1.048	65.3901

Comp61	3'- F	CH <sub>2</sub> CH <sub>3</sub>	6.167	6.425	-0.258	60.914
Comp62	3'- F	CH <sub>2</sub> CH=CH <sub>2</sub>	5.287	6.050	-0.763	55.0781
Comp63	3'- F	(CH <sub>2</sub> ) <sub>2</sub> F	5.757	6.293	-0.536	59.9575
Comp64	3'- F	(CH <sub>2</sub> ) <sub>2</sub> OH	5.446	5.729	-0.283	55.404
<b>*Comp65</b>	<b>3'- F</b>	<b>(CH<sub>2</sub>)<sub>3</sub>OH</b>	<b>6.01</b>	*****	*****	*****
Comp66	2'- Cl	CH <sub>2</sub> C≡CH	7.131	6.818	0.313	59.7118
Comp67	2'- Cl	CH <sub>2</sub> CH <sub>3</sub>	6.921	6.024	0.897	57.9843
Comp68	2'- CF <sub>3</sub>	CH <sub>2</sub> C≡CH	6.319	5.928	0.391	53.5381
Comp69	2'- CH <sub>3</sub>	CH <sub>2</sub> C≡CH	6.301	6.513	-0.212	72.9112
Comp70	2'- CH <sub>3</sub>	CH <sub>3</sub>	6.027	6.416	-0.389	65.5774
Comp71	2'- CH <sub>3</sub>	CH <sub>2</sub> CH <sub>3</sub>	6.495	5.912	0.583	56.4926
Comp72	2'- NH <sub>2</sub>	CH <sub>2</sub> C≡CH	6.538	6.437	0.101	61.8012
Comp73	2'- NH <sub>2</sub>	CH <sub>3</sub>	6.066	5.913	0.153	74.1392
Comp74	2'- NH <sub>2</sub>	CH <sub>2</sub> CH <sub>3</sub>	6.509	6.634	-0.125	67.3791
Comp75	2'- OH	CH <sub>2</sub> C≡CH	7.046	7.218	-0.172	79.6766
Comp76	2'- OCH <sub>3</sub>	CH <sub>2</sub> C≡CH	7.174	6.829	0.345	63.4102
Comp77	2'- OCH <sub>3</sub>	CH <sub>2</sub> CH <sub>3</sub>	6.721	7.250	-0.529	55.2489
Comp78	2'- NO <sub>2</sub>	CH <sub>2</sub> C≡CH	6.886	5.945	0.941	52.9612
Comp79	2'- NO <sub>2</sub>	CH <sub>2</sub> CH <sub>3</sub>	6.84	6.226	0.613	47.4045



	Position R	Position Ar				
Comp80	CH <sub>2</sub> C≡CH		6.357	6.757	-0.400	54.2254
Comp81	H		4.606	5.323	-0.717	69.7193
Comp82	CH <sub>3</sub>		6.174	6.413	-0.239	88.1727
Comp83	CH <sub>2</sub> CH <sub>3</sub>		6.237	6.089	0.148	65.42
Comp84	(CH <sub>2</sub> ) <sub>2</sub> CH <sub>3</sub>		5.733	5.928	-0.195	27.2274
Comp85	CH <sub>2</sub> CH=CH		5.755	6.137	-0.382	57.8916
Comp86	(CH <sub>2</sub> ) <sub>2</sub> F		6.26	6.377	-0.117	58.3581
Comp87	(CH <sub>2</sub> ) <sub>2</sub> OH		5.921	6.227	-0.306	68.9653



Comp88	(CH <sub>2</sub> ) <sub>3</sub> OH		5.474	6.456	-0.982	67.2375
Comp89	CH <sub>2</sub> CN		5.511	6.117	-0.606	70.8413
Comp90	CH <sub>2</sub> C≡CH		6.638	7.039	-0.401	56.7366
Comp91	H		5.148	5.726	-0.578	77.5187
Comp92	CH <sub>3</sub>		6.377	5.844	0.533	76.4319
Comp93	CH <sub>2</sub> CH <sub>3</sub>		6.638	6.152	0.486	70.5299
Comp94	CH <sub>2</sub> CH=CH <sub>2</sub>		5.971	5.863	0.108	49.9632
Comp95	(CH <sub>2</sub> ) <sub>2</sub> F		6.721	6.714	0.007	52.658
Comp96	(CH <sub>2</sub> ) <sub>2</sub> OH		6.377	6.122	0.255	69.8192
Comp97	(CH <sub>2</sub> ) <sub>3</sub> OH		5.759	6.239	5.67	0.09
Comp98	CH <sub>2</sub> CH <sub>3</sub>		6.119	6.672	6.14	-0.02
Comp99	CH <sub>2</sub> CH <sub>3</sub>		6.027	5.790	6.00	0.03
Comp100	CH <sub>2</sub> C≡CH		7.398	6.506	7.18	0.22
Comp101	CH <sub>3</sub>		6.456	6.150	5.61	0.85
Comp102	CH <sub>2</sub> CH <sub>3</sub>		6.824	6.812	6.65	0.17
Comp103	CH <sub>2</sub> CH=CH <sub>2</sub>		6.119	6.364	5.93	0.19
*Comp104	(CH <sub>2</sub> ) <sub>2</sub> F		<b>6.8</b>	*****	*****	*****
*Comp105	CH <sub>3</sub>		<b>5.37</b>	*****	*****	*****
*Comp106	CH <sub>3</sub>		<b>5.63</b>	*****	*****	*****

\* Outlier